Comparison of two soil temperature algorithms for a bare ground site on the Loess Plateau in China

Zhiqiu Gao,[1] Donald H. Lenschow,[2] Robert Horton,[3] Mingyu Zhou,[1,4] Linlin Wang,[1] and Jun Wen[5]

[1]   Two thermal transfer algorithms for soil are used to investigate the diurnal vertical temperature variation in the common case of a vertically heterogeneous thermal diffusivity and the considerable liquid water flux which generally exists in soil when surface evaporation is large. One algorithm assumes that soil is vertically homogenous and takes into account only thermal conduction, and the other, developed in our recent study, considers the vertical heterogeneity of thermal diffusivity in soil and couples thermal conduction and convection (e.g., heat transfer by water flux). Theoretically the two methods are identical for vertically homogenous dry soil. On the basis of soil temperature data collected at a bare soil site over the Loess Plateau of China during the period from DOYs 197 to 241, 2005, we found that the new algorithm gives a realistic estimate of soil temperature while the previous one, on average, overestimates either the diurnal amplitude by 0.95 K or the phase shift by 0.207 rad (i.e., 47.44 min) at the soil depth of 0.10 m. Using the new algorithm and measurements of soil temperature, we determine the soil thermal diffusivity and a variable that represents the sum of the vertical gradient of soil thermal diffusivity and water flux density at three levels within the first 0.40 m of the soil surface. We also simulate the soil temperature for the depths of 0.20 m and 0.40 m, and the results are in satisfactory agreement with direct measurements. The main contribution here is to provide analytic insight into the role of heterogeneity and some simple formulae as tools for interpretation of the role of heterogeneity in observed diurnal temperature variations.

1.   Introduction

[2] Surface temperature and soil moisture content are important hydrologic parameters which affect exchanges of sensible and latent heat between the atmosphere and the land surface, which in turn affect soil temperature. In the early literature, the temperature of homogeneous soil was derived as a solution of the heat diffusion equation with a constant diffusivity in a semi-infinite medium under periodic forcing at the soil surface [*Van Wijk and de Vries*, 1963]. *Nerpin and Chudnovskii* [1984] examined the periodic temperature variations in an inhomogeneous soil where the thermal properties were described by linear profiles. *Novak* [1986] calculated the effective daily atmo-

spheric and soil thermal admittances by using harmonic solutions to the one-dimensional heat transfer equation for a semi-infinite medium. The thermal properties of both media were assumed to be power functions of depth only and he showed how to calculate the parameters in these functions. Later, *Novak* [1991] proposed a new analytical theory that accounts for aperiodic transient effects and compared his predictions with measured soil temperatures. His theory also accounts for the observed soil warming trend but is sensitive to small errors in the prescribed soil surface heat flux. *Massman* [1993] examined periodic temperature variations in an inhomogeneous soil where the thermal properties were prescribed by exponential profiles.

[3] More recently, soil heat transfer has been shown to be caused by a complex combination of conductive processes and intraporous convective processes [e.g., *Passerat de Silans et al.*, 1996], which has led to the development of solutions for the thermal conduction-convection equation. Examples of results using such a model are given by *Shao et al.* [1998], *Ren et al.* [2000], and *Gao et al.* [2003]. *Shao et al.* [1998] compared analytical results with data collected during a field infiltration experiment involving natural diurnal variations of soil temperature and showed that the predicted temperatures were very similar to the direct

---

[1]State Key Laboratory of Atmospheric Boundary Layer Physics and Atmospheric Chemistry, Institute of Atmospheric Physics, CAS, Beijing, China.

[2]National Center for Atmospheric Research, Boulder, Colorado, USA.

[3]Department of Agronomy, Iowa State University, Ames, Iowa, USA.

[4]Also at Key Laboratory for Polar Science, Polar Research Center of China, Shanghai, China.

[5]Cold and Arid Regions Environmental and Engineering Research Institute, CAS, Lanzhou, China.

measurements. *Ren et al.* [2000] presented a method to determine soil water flux and pore-water velocity by a heat-pulse technique. Their method improved upon earlier methods by reducing distortion of the water flow field and minimizing heat-induced soil water redistribution. *Karam* [2000] developed a novel thermal wave model based on the wave-like characteristics of periodic heat flow for studying heat transfer in nonuniform soils. *Gao et al.* [2003] solved analytically the equation for one-dimensional thermal conduction-convection in vertically homogenous soil by applying the harmonic method. *Verhoef et al.* [1996] examined soil thermal diffusivity at the HAPEX-Sahel site (Africa) by using five methods and *Verhoef* [2004] presented a method to estimate thermal inertia (the soil capacity times the square root of the soil thermal diffusivity) remotely from micrometeorological measurements. *Massman and Frank* [2004] measured soil temperatures and heat fluxes at several soil depths before, during, and after a controlled surface burn at Manitou Experimental Forest (southern Colorado, USA) to evaluate its effects on the soil's thermophysical properties (thermal conductivity and volumetric specific heat capacity). During the burn the soil was heated to over $400°C$ at a depth of 0.02 m and to almost $100°C$ at 0.30 m. Relatively high temperatures persisted for several hours to days even over 1 m deep into the soil. They found that soil thermophysical properties, estimated before and after the fire with a new model of periodic heat flow in soils, were not significantly changed between the times shortly after sensor installation (October 2001) and 1 month after the fire (February 2002). Furthermore, *Massman et al.* [2008] examined long-term changes in the soil temperature and heat fluxes resulting from fire by developing and using an analytical model of the daily and annual cycles of soil heating and cooling. Their modeling results suggest that under dry soil conditions typical of the experimental forest, the amplitudes of the daily and seasonal cycles of soil heating/cooling in the fire-affected soils greatly exceeded those in the soils unaffected by fire for several months to years following the fire and that these effects propagate to depths exceeding a meter. These studies typify the latest developments in determining soil temperature distribution.

[4] Recently, *Holmes et al.* [2008] applied two field data sets to models of near-surface soil temperature profiles in bare soil. They showed that the commonly used solutions to the heat flow equations by *Van Wijk and de Vries* [1963] perform well when applied to deeper soil layers, but resulted in large errors when applied to near-surface layers, where more extreme variations in temperature occur. Their explanation is that these approaches do not consider heat sources or sinks below the surface.

[5] The land-air interaction over the Loess Plateau located in midwestern China affects the weather and climate in northwest China [*Wang*, 2004]. In the Simple Biosphere Model 2 (hereinafter, referred to as SiB2) which has been frequently used in GCMs [*Randall et al.*, 1996] for estimating global land surface turbulent fluxes, soil surface temperature is calculated by using the surface energy balance equation, i.e., the force-restore method. After soil surface temperature is determined and taken as the upper boundary condition, soil temperature in deeper layers is estimated by using the traditional thermal conduction equation where the soil thermal diffusivity is parameterized

by using soil volumetric water content [*Sellers et al.*, 1996] and the impact of vertical water flux on soil temperature is neglected. Few presentations have been made regarding soil thermal properties and temperature distribution in bare soil on the Loess Plateau. To satisfy these needs, this paper quantifies the soil heat diffusivity over the Loess Plateau, and compares two algorithms for estimating soil temperature using the data collected during the Loess Plateau land surface process field Experiment (LOPEX) in 2005. The first algorithm, widely used in the early literature, assumes that soil is vertically homogenous and takes into account only thermal conduction. The other algorithm, developed from the work by *Gao et al.* [2003], considers the vertical heterogeneity of thermal diffusivity in soil and couples thermal conduction and convection (e.g., heat transfer by water flux).

2. Review and Comparison of the Two Algorithms

2.1. Classical Thermal Conduction Equation for Soil Temperature

[6] Following *Van Wijk and de Vries* [1963], we utilize the fundamental periodic solution of the heat diffusion equation

$$\partial T/\partial t = k\partial^2 T/\partial z^2, \qquad (1)$$

where k is the thermal diffusivity and $k \equiv \lambda/C_g$ where λ is the thermal conductivity and C_g is the volumetric heat capacity of the soil. Given the boundary condition at a depth z_2: $T \mid_{z=z_2} = \overline{T_2} + A_2 \sin(\omega t - \Phi_2)$ with $t \geq 0$, the soil temperature (T) at a depth z_1 can be calculated via

$$T(z_1, t) = \overline{T_1} + A_2 \exp[-(z_1 - z_2)\alpha] \sin[\omega t - \Phi_2 - (z_1 - z_2)\alpha], \qquad (2)$$

where z is the vertical coordinate positive downward, t the time; $\overline{T_1}$ and $\overline{T_2}$ are the arithmetical averages of the daytime maximum soil temperature and the nighttime minimum soil temperature, and A_2 is half of the difference between the daytime maximum value and the nighttime minimum value for soil depth of z_2; ω is the angular velocity of the Earth's rotation; Φ_2 is the initial phase of soil temperatures at depth z_2, obtained by using the best approach method [*Gao et al.*, 2003]; and $\alpha \equiv \sqrt{\omega/2k}$, where α^{-1} is the damping depth of the diurnal temperature wave. Equation (2) implies that the amplitude of the soil temperature wave exponentially decreases and its phase linearly increases for increasing soil depth. If the mean temperature profile is given, the only unknown parameter is the soil thermal diffusivity.

2.2. Soil Temperature Rate Equation With Vertical Heterogeneity of Soil Thermal Diffusivity Coupled With Thermal Conduction and Heat Transfer by Water Flux

[7] Equation (1) assumes that the soil is vertically homogeneous. But k can vary (increase or decrease) from the surface downward in a shallow layer for most soils. Equation (1) can therefore be improved as follows:

$$\frac{\partial T}{\partial t} = \frac{1}{C_g} \frac{\partial}{\partial z} \left(\lambda \frac{\partial T}{\partial z} \right) = \frac{\lambda}{C_g} \frac{\partial^2 T}{\partial z^2} + \frac{1}{C_g} \frac{\partial \lambda}{\partial z} \frac{\partial T}{\partial z}$$
$$\approx k \frac{\partial^2 T}{\partial z^2} + \frac{\partial k}{\partial z} \frac{\partial T}{\partial z}. \qquad (1')$$

Neglecting the vertical heterogeneity of k, *Gao et al.* [2003] incorporated thermal conduction and convection together as follows:

$$\frac{\partial T}{\partial t} = k\frac{\partial^2 T}{\partial z^2} - \frac{C_W}{C_g}w\theta\frac{\partial T}{\partial z}, \tag{1''}$$

where w is the liquid flow rate (positive downward) and θ is the volumetric water content of the soil. C_w is the heat capacity of water. These four quantities are assumed independent of z for a thin soil layer in the present work. $-\frac{C_W}{C_g}w\theta$ was defined as water flux by *Gao et al.* [2003].

[8] Combining equations (1′) and (1″),

$$\frac{\partial T}{\partial t} = k\frac{\partial^2 T}{\partial z^2} + W\frac{\partial T}{\partial z}, \tag{3}$$

where, $W \equiv \frac{\partial k}{\partial z} - \frac{C_W}{C_g}W\theta$. One can see that w consists of two parts: (1) $\frac{\partial k}{\partial z}$, the vertical gradient of soil diffusivity and (2) $-\frac{C_W}{C_g}w\theta$, the water flux density. Similar to *Gao et al.* [2003], given the boundary condition mentioned above, the solution to equation (3) is

$$T(z_1, t) = \overline{T_1} + A_2\exp[-(z_1 - z_2)\alpha M]$$
$$\cdot \sin[\omega t - \Phi_2 - (z_1 - z_2)\alpha N], \tag{4}$$

where $M = \frac{\alpha}{\omega}\{W + \frac{1}{\sqrt{2}}[W^2 + (W^4 + \frac{4\omega^4}{\alpha^4})^{1/2}]^{1/2}\}$ and $N = \sqrt{2}(\frac{\omega}{\alpha})[W^2 + (W^4 + \frac{4\omega^4}{\alpha^4})^{1/2}]^{-1/2}$. Comparing equation (4) with equation (2), M and N are the additional terms obtained from the solution to equation (3). It must be noted that equation (4) is really not a solution to the equation with variable k but is expected to adequately approximate the solution over a layer over which k does not vary too much.

[9] We let $A_1 = A_2\exp[-(z_1 - z_2)M]$ and $\Phi_1 = \Phi_2 + \alpha(z_1 - z_2)N$. Then Φ_1 and Φ_2 are initial phases of soil temperatures at the depths z_1 and z_2, respectively. Assuming $z_1 > z_2$ (i.e., $A_1 < A_2$ and $\Phi_1 > \Phi_2$), *Gao* [2005] derived the followed equations:

$$k = -\frac{(z_1 - z_2)^2\omega\ln(A_1/A_2)}{(\Phi_1 - \Phi_2)\left[(\Phi_1 - \Phi_2)^2 + \ln^2(A_1/A_2)\right]}, \tag{5}$$

$$W = \frac{\omega(z_1 - z_2)}{\Phi_1 - \Phi_2}\left[\frac{-(\Phi_1 - \Phi_2)^2 + \ln^2(A_1/A_2)}{(\Phi_1 - \Phi_2)^2 + \ln^2(A_1/A_2)}\right]$$
$$= \frac{\omega(z_1 - z_2)}{\Phi_1 - \Phi_2}\left[\frac{2\ln^2(A_1/A_2)}{(\Phi_1 - \Phi_2)^2 + \ln^2(A_1/A_2)} - 1\right]. \tag{6}$$

2.3. Theoretical Comparison Between the Two Soil Temperature Rate Equations

[10] A comparison between equation (4) and equation (2) shows the following.

[11] 1. The solutions to equations (2) and (4) are identical for vertically homogenous dry soil where $W = 0$ because $\partial k/\partial z = 0$ for vertically homogenous soil and $-\frac{C_W}{C_g}w\theta = 0$ for dry soil. Applying $W = 0$ to equation (6) results in

$$\Phi_2 - \Phi_1 = -\ln(A_2/A_1) = \ln(A_1/A_2) = -(z_1 - z_2)\alpha, \tag{7}$$

and applying equation (7) to equation (5) results in

$$k = (z_1 - z_2)^2\omega/[2(\Phi_1 - \Phi_2)^2], \tag{8}$$

or

$$k = (z_1 - z_2)^2\omega/[2\ln^2(A_1/A_2)]. \tag{9}$$

Equations (8) and (9) are the standard equations given by *Horton et al.* [1983], who called them the phase and amplitude methods, respectively. Equation (8) allows soil thermal diffusivity to be calculated by using the phase difference of soil temperatures at two depths, and equation (9) shows that soil thermal diffusivity can be calculated from the amplitude ratio of soil temperatures at two depths. Because $A_1 \neq A_2$, $\Phi_1 \neq \Phi_2$ and $z_1 \neq z_2$, $k > 0$ always, equations (7)–(9) imply that for vertically homogenous dry soil: (1) the phase shift is equal to the logarithm of the amplitude ratio of soil temperatures at two depths; (2) thermal conduction still occurs whereas convection does not; and (3) soil thermal diffusivity k can be determined using either amplitudes or phases of soil temperatures collected at two depths.

[12] 2. Equation (2) shows that for any vertically homogenous dry soil layer of thickness $(z_1 - z_2)$: $\Phi_2 - \Phi_1 = \ln(A_1/A_2) = -\alpha(z_1 - z_2)$. However, for a soil layer where $W \neq 0$, equation (4) gives $\ln(A_1/A_2) = -(z_1 - z_2)\alpha M$ and $\Phi_2 - \Phi_1 = -(z_1 - z_2)\alpha N$. When $W > 0$, $\ln(A_1/A_2) < \Phi_2 - \Phi_1 < 0$, and when $W < 0$, $0 > \ln(A_1/A_2) > \Phi_2 - \Phi_1$.

[13] 3. For $W > 0$, if soil thermal diffusivity is estimated from equation (8) to be, say, k_1, it will be overestimated. Equation (2) therefore will overestimate the soil temperature amplitude, because $0 > -(z_1 - z_2)\sqrt{\omega/2k_1} > -(z_1 - z_2)\alpha M$. Physically, this is easy to understand. For example, for a vertically homogenous wet soil layer with significant evaporation at the soil surface at noon during clear days, the warm liquid water stored near the surface will evaporate and the cold liquid water beneath will flow upward toward the surface, so the surface layer will become cooler [*Gao*, 2005]. Equation (2) does not account for this process, so it will generate a warmer surface layer under these conditions.

[14] 4. If k is estimated from equation (9) to be, say, k_2, it will be underestimated. Equation (2) will overestimate the phase shift of soil temperature, because the inequality, $-(z_1 - z_2)\sqrt{\omega/2k_2} < -(z_1 - z_2)\alpha N < 0$, will always hold whether $W > 0$ or $W < 0$.

3. Field Experiments

[15] The data used here were collected at a bare soil site on the Loess Plateau during an intensive observation period from DOYs 197 to 241 in LOPEX in 2005. This site, designed for quantifying the land-atmosphere interaction at the bare soil surface, was located at 106.42°E, 35.35°N at an altitude of 1592 m in Pingliang county of Gansu Province in western China. The ground surface was bare, flat and homogeneous. The soil at the site was predominantly medium loam with a high proportion of silt. The site is located within a semiarid climate zone. The maximum air temperature was 307 K and the lowest was 249 K, the annual air temperature and precipitation were 279 K and
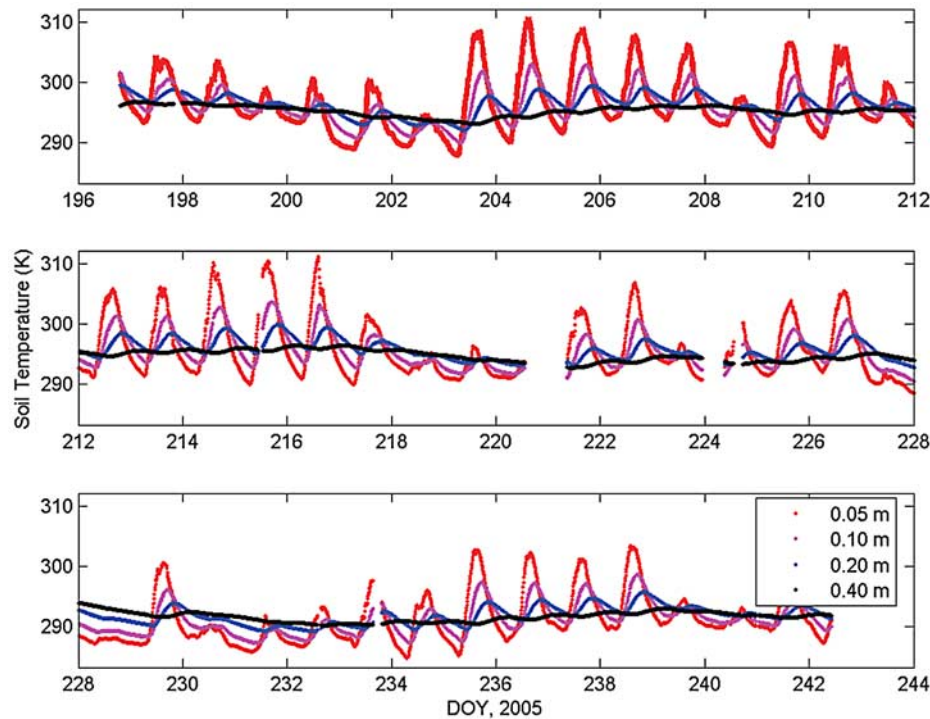
Figure 1. Temporal variations of soil temperature (K) measured at depths of 0.05 m, 0.10 m, 0.20 m, and 0.40 m at a bare soil site on the Loess Plateau from DOY 197 through DOY 241, 2005.

510 mm with 2425 hours of sunshine, and 170 frost-free days per year all averaged over the last 50 years [*Wei et al.*, 2005].

[16] Soil temperature and volumetric water content were measured at 0.05 m, 0.10 m, 0.20 m, and 0.40 m depth, and all of the sensor outputs were recorded and averaged over 10 min intervals, by Campbell (Campbell Scientific Inc.) TCAV-averaging Soil Thermocouple Probes and CS615 Soil Moisture Reflectometers, respectively.

[17] Standard micrometeorological measurements were also made at the site, including four radiation components, wind speed, wind direction, air temperature, air relative humidity, air pressure and precipitation. We do not include the micrometeorological measurements here for brevity.

4. Results and Discussion

[18] Figure 1 shows the diurnal variation in soil temperatures measured at 0.05 m, 0.10 m, 0.20 m, and 0.40 m depths at the bare soil site throughout the experimental period. The diurnal cycle at shallow depth is larger than that at greater depths so that the soil temperature at a shallow level was higher (lower) than that at a deeper level in daytime (nighttime). Only the soil temperature collected at 0.05 m changed in response to the intermittent cloudiness. The maximum (minimum) soil temperature reached 311.13 K (284.66 K) at 0.05 m depth during the experimental period. The amplitude of the soil temperature cycle decreased and the phase of the soil temperature shifted ahead when the soil depth increased. Figure 1 also shows that the soil vertical temperature gradient reached 191.20 K m^{-1} for the soil layer from 0.05 to 0.10 m at 1445 local time (hereinafter referred to as LT) on DOY 204 at this site. Such

large vertical temperature gradients generally exist in soil with a bare surface owing to large daytime solar heating. This is the nature of the uncultivated areas on the Loess Plateau.

[19] *Heusinkveld et al.* [2004] directly measured the soil temperature distribution in a sandy desert belt situated northwest of Negev, Israel, and showed that the amplitude of the diurnal variation at 0.10 m depth was larger than 7 K. The amplitude of diurnal variation reached 10.5 K and 5.5 K respectively at 0.05 m and 0.10 depths at our site. The diurnal variation of soil temperature amplitude rapidly decreased with increasing depth and it was almost constant at 0.40 m depth.

[20] Figure 2 is same as Figure 1 but for soil volumetric water content. The abrupt increases in soil volumetric water content at 0.05 m depth occurred at the moment when precipitation occurred. The gaps in Figures 1 and 2 are caused by problems in the collection equipment.

4.1. Estimates of Soil Thermal Diffusivity *k* and the Sum(*W*) of the Vertical Gradient of Soil Thermal Diffusivity and Water Flux Density

[21] In reality, the soil temperature distribution depends on many factors, such as absorbed radiation energy, cloud cover, and some internal physical processes [*Gao et al.*, 2003]. In our analysis above, for simplicity, we assumed the soil temperature varies sinusoidally. After using a 2-hour smoothing technique for soil temperature measured at a depth of 0.05 m, we applied the sine function, $T_2 = \overline{T_2} + A_2 \sin(\omega t - \Phi_2)$, to best approximate the curve of soil temperature collected at the depth of 0.05 m, and applied the sine function, $T_1 = \overline{T_1} + A_1 \sin(\omega t - \Phi_1)$, to approximate the curve of soil temperature collected at the depth of
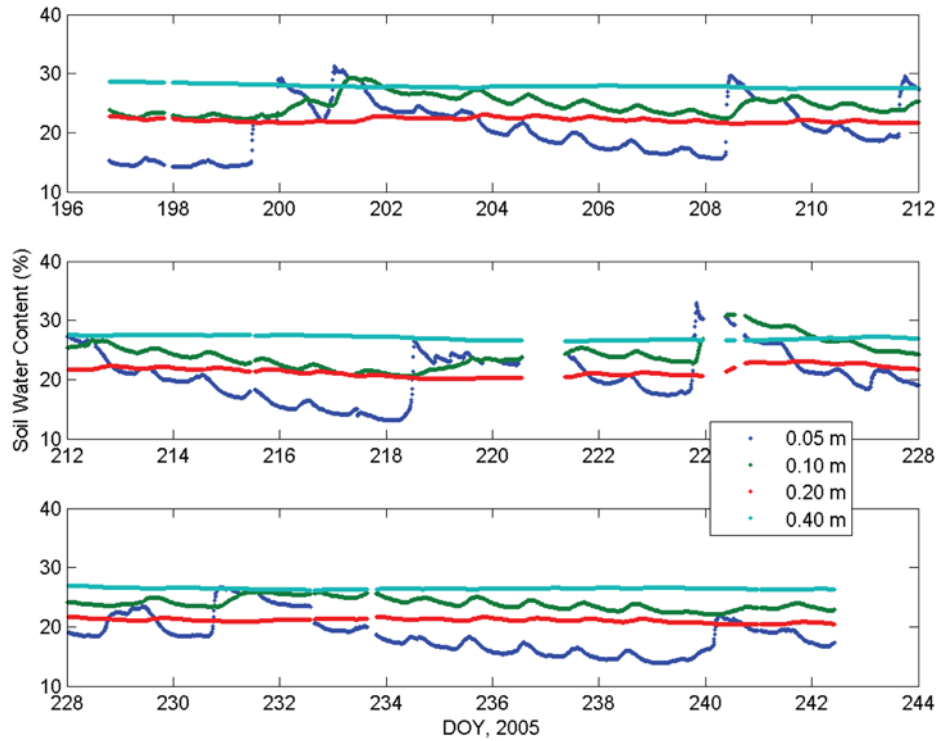
Figure 2. Temporal variations of soil volumetric water content (m^3 m^{-3}) measured at depths of 0.05 m, 0.10 m, 0.20 m, and 0.40 m at a bare soil site on the Loess Plateau from DOY 197 through DOY 241, 2005.

0.10 m for each day, respectively. The temporal variations of k and W are therefore obtained by using equations (5) and (6) for three soil layers: from 0.05 m to 0.10 m, from 0.10 m to 0.20 m, and from 0.20 m to 0.40 m in Figure 3. On average for the three layers, $k = 3.70 \times 10^{-7}$ m^2 s^{-1}, $k = 6.54 \times 10^{-7}$ m^2 s^{-1}, and $k = 2.55 \times 10^{-7}$ m^2 s^{-1}, respectively. It is obvious that k is vertically heterogeneous; it first increases just below the surface and then decreases dramatically downward at our site. As shown above, k is determined by using equation (5) where the amplitudes and phases of soil temperature measured at two depths are used, which means that equation (5) assumes obvious diurnal variations in soil temperatures at two depths. Figure 1 shows that the diurnal variation in soil temperature at 0.4 m depth is not significant. The complication of determining the amplitude and phase of soil temperature at this depth would cause uncertainties in k regardless of how carefully it was estimated. *Garratt* [1992] presented some representative values of thermal diffusivity. The values obtained here for the top two layers are close to his value for thermal diffusivity of clay soil with a volumetric soil water content of 20% (5.2×10^{-7} m^2 s^{-1}).

[22] For this same case, $W = 1.65 \times 10^{-6}$ m s^{-1}, $W = 1.01 \times 10^{-6}$ m s^{-1}, and $W = -2.40 \times 10^{-6}$ m s^{-1}. As given above, $W = \partial k/\partial z - (C_W/C_g)w\theta$, where w is usually expected to be only a few millimeters per day of evaporation flux, and the soil water flux, $(C_W/C_g)w\theta$, responds to the evaporation boundary condition so one can also expect only a few millimeters per day soil water flux. Thus, $(C_W/C_g)w\theta$ is about half of $\partial k/\partial z$, and $\partial k/\partial z$ is the main contributor to W.

[23] *Shao et al.* [1998] assumed that water flux density (W) is periodic,

$$\frac{\partial T}{\partial t} = k\frac{\partial^2 T}{\partial z^2} + [a + b\sin(\omega t)]\frac{\partial T}{\partial z}, \qquad (10)$$

where a and b are constants with dimensions of W, and derived an analytical solution to the problem. In their work, there were two separate integral processes incorporated in the analytical solution and the method requires not only the soil surface temperature, but also the initial soil temperature profile, which would complicate its use in numerical models. Our analytical solution (i.e., equation (4)) is more practical, as it requires only soil surface temperature.

[24] Because $W \neq 0$ for our site and the previous method (i.e., equation (2)) does not account for W, we expect that the new method (i.e., equation (4)) is better than the previous method for modeling soil temperature at our site.

[25] Figure 4 shows the variations of soil thermal diffusivity k and W with the volumetric soil water content θ. We see that neither k nor W change over a narrow range of volumetric soil water content. *Verhoef et al.* [1996] found that k increased with increasing volumetric soil water content for the data collected during the HAPEX-Sahel experiment in 1992. *Gao* [2005] found that both k and W increased with increasing volumetric soil water content for the data collected during the GAME/Tibet experiment in 1998. Our results are not the same as with the Tibetan prairie case because the change in soil heat diffusivity with depth is influenced by the soil water content profile as well as soil texture, and the soil contains a quite large percentage
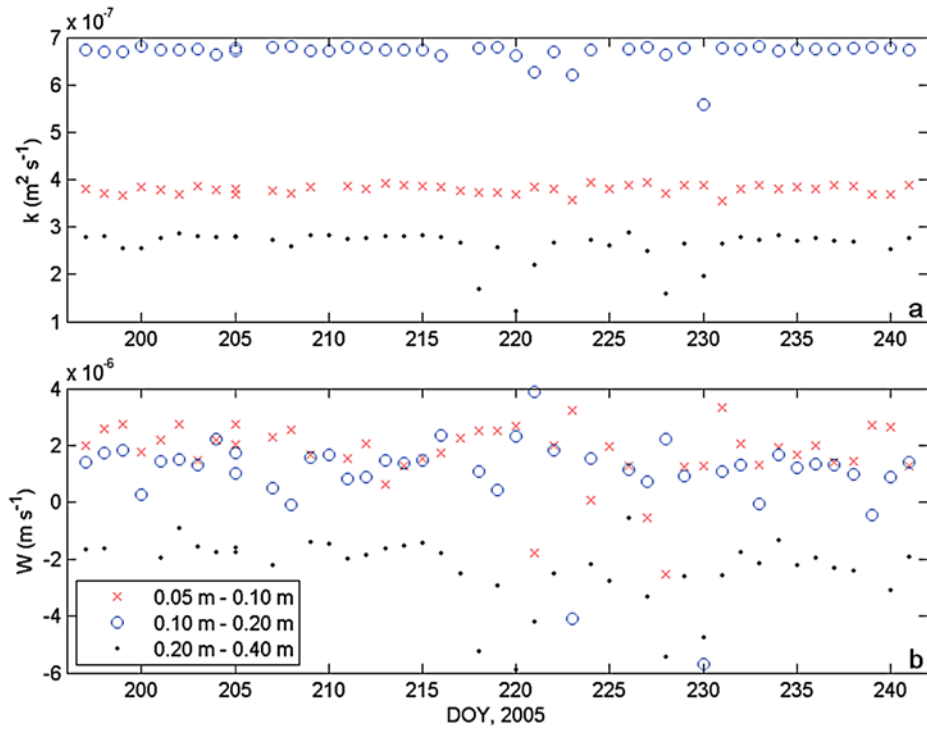
Figure 3. Temporal variation of (a) soil thermal diffusivity k (m^{-2} s^{-1}) and (b) $W(= \frac{\partial k}{\partial z} - \frac{C_W}{C_g}w\theta)$ (m s^{-1}) at a bare soil site on the Loess Plateau from DOY 197 through DOY 241, 2005.
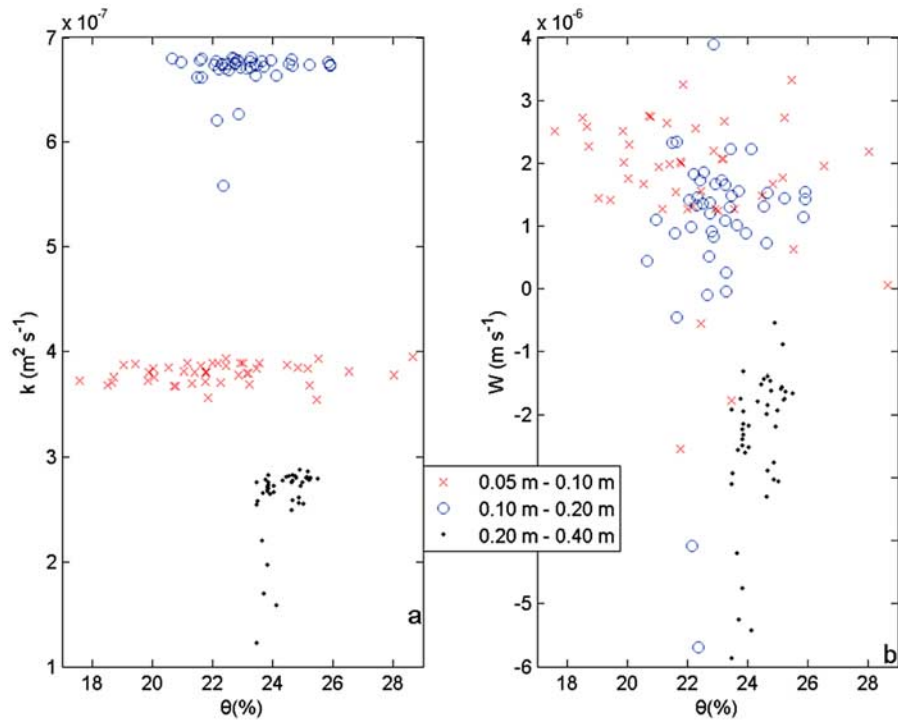

Figure 4. Variation of (a) soil thermal diffusivity k (m^2 s^{-1}) and (b) $W(= \frac{\partial k}{\partial z} - \frac{C_W}{C_g}w\theta)$ (m s^{-1}) with volumetric soil water content θ (%) at a bare soil site on the Loess Plateau from DOY 197 through DOY 241, 2005.

Figure 5. Comparisons of the observed temperature at a depth of 0.10 m from DOY 197 to DOY 241, 2005, with soil temperature modeled by using: (1) equation (4), where k and W are calculated with equations (5) and (6); (2) equation (2) where k is calculated with equation (8) and $W = 0$; and (3) equation (2) where k is calculated with equation (9) and $W = 0$.

of roots at the Tibetan site which is very different from the soil on the Loess Plateau.

4.2. Comparison Between the Logarithmic Amplitude Attenuation $\ln(A_1/A_2)$ and the Phase Shift $\Phi_2 - \Phi_1$

[26] For the study period, the logarithmic amplitude attenuation, $\ln(A_1/A_2) = -0.60$, and phase shift $\Phi_2 - \Phi_1 = -0.48$. The fact that $\ln(A_1/A_2) < \Phi_2 - \Phi_1$ illustrates the problem of using equation (2) for modeling soil temperature at this site because equation (2) assumes $\ln(A_1/A_2) = \Phi_2 - \Phi_1$. In fact, $\ln(A_1/A_2) < \Phi_2 - \Phi_1$ agrees with the theoretical analysis (for $W > 0$) given in section 2.3 above.

4.3. Comparison of Two Methods for Modeling of Soil Temperature

[27] Because both k (i.e., soil thermal diffusivity) and W (i.e., the sum of the vertical gradient of soil thermal diffusivity and water flux density) are determined, soil temperature at a depth of 0.10 m can be modeled by using soil temperature measured at 0.05 m depth in equation (4). In reality, the soil temperature contains many harmonic waves. We simply assumed that soil temperature measured at the 0.05 m depth has a single sinusoidal component, because it helps us obtain an analytical solution (i.e., equation (4)). To avoid possible serious errors introduced by this assumption, we separated the process of modeling soil temperature at 0.10 m depth by using equation (4) in two steps as follows: (1) shifting the phase of soil temperature measured at 0.05 m depth by $-(z_1 - z_2)\alpha N$, and (2) multiplying the magnitude of soil temperature measured at 0.05 m depth by $\exp(-(z_1 - z_2)\alpha M)$. The results are

given in Figure 5. Overall, equation (4) generates a realistic soil temperature amplitude for the daytime. However, equation (4) underestimates the soil temperature during the period from 1800 LT to 0800 LT, and a noteworthy difference (up to 1.3 K) between the measurements and the model output occurred around 0200 LT for all days in our research period. This underestimation was also encountered by *Lin* [1980]. The reasons are complicated, because the model results depend on the initial soil moisture content, hydraulic conductivity and hydraulic potential gradient. In equation (4) we applied the observed soil temperature shift of -0.48 rad in evaluations of k and W.

[28] We also model soil temperature at 0.10 m depth by using equation (2) where W is neglected. Because $\ln(A_1/A_2) \neq \Phi_2 - \Phi_1$, there are two options (i.e., equation (8) or equation (9)) for determining k, leading to $k = 3.94 \times 10^{-7}$ m^2 s^{-1}, and $k = 2.44 \times 10^{-7}$ m^2 s^{-1}, respectively. The corresponding values of soil temperature modeled by using these two values of k are also given in Figure 5. Comparison of modeled results against the direct measurement shows the following.

[29] 1. When k was estimated to be 3.94×10^{-7} m^2 s^{-1} by using equation (8), equation (2) overestimates soil temperature amplitude by 0.95 K on average for our experimental period, but makes a realistic estimate of the soil temperature phase shift as shown in Figure 5. Using equation (8) to determine k implies forcing $\ln(A_1/A_2)$ to be equal to $\Delta\Phi$ ($\equiv \Phi_2 - \Phi_1$), which overestimates the soil temperature amplitude. To better show the difference between model outputs and measurements, we plot the results for a clear day, DOY 204, in Figure 6. Further, the
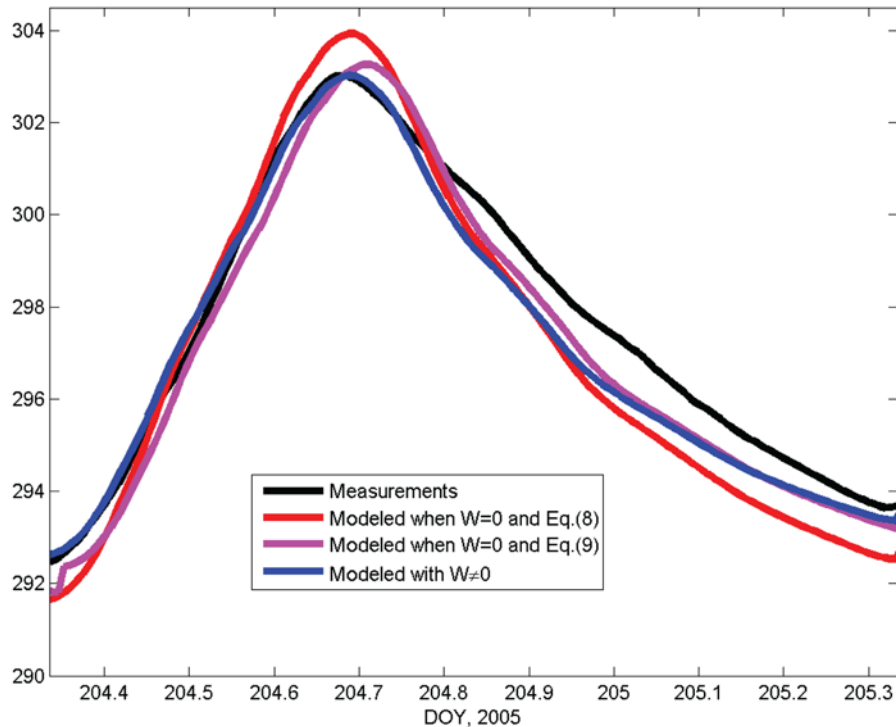
Figure 6. Comparison of the observed temperature at a depth of 0.10 m on DOY 204, 2005 with soil temperature modeled by using: (1) equation (4) where k and W are calculated with equations (5) and (6); (2) equation (2) where k is calculated with equation (8) and $W = 0$; and (3) equation (2) where k is calculated with equation (9) and $W = 0$.

variations of k and W against ln (A_1/A_2) are given in Figure 7. It is obvious that when $\Delta\Phi$ is fixed to be -0.48 rad, k (W) increases (decreases) with increasing ln (A_1/A_2) under the condition ln $(A_1/A_2) < -0.48$. When ln (A_1/A_2) reaches -0.48, $W = 0$ and k reaches the maximum value of 3.94×10^{-7} m^2 s^{-1}. We also plot the results (open circles) of k and W for the experimental period obtained by using equations (5) and (6) in Figure 7. Comparing the average $k(= 3.70 \times 10^{-7}$ m^2 s$^{-1})$ with $k(= 3.94 \times 10^{-7}$ m^2 s$^{-1})$ obtained by using equation (8) shows that equation (8) overestimates k, directly causing an overestimate in the soil temperature amplitude from equation (2).

[30] 2. When k was estimated to be 2.44×10^{-7} m^2 s^{-1} by using equation (9), equation (2) reasonably estimates the soil temperature amplitude, but overestimates the phase shift of 0.207 rad ($\approx$47.44 min) as shown in Figures 5 and 6. Using equation (9) to determine k implies forcing $\Delta\Phi$ to be equal to $\ln(A_1/A_2)$, which overestimates the soil temperature phase shift of $\Delta\Phi - \ln(A_1/A_2) = 0.207$ rad. To help understand this result, the variations of k and W against $\Delta\Phi$ are given in Figure 8. It is obvious that when $\ln(A_1/A_2)$ is fixed to be -0.60, both k and W increase with increasing $\Delta\Phi$. When $\Delta\Phi$ is decreased to -0.60, $W = 0$ and $k = 2.44 \times 10^{-7}$ m^2 s^{-1}. We also plot the averaged results of $k(= 3.70 \times 10^{-7}$ m^2 s$^{-1})$ and $W(= 1.65 \times 10^{-6}$ m s$^{-1})$ obtained by using equations (5) and (6) in Figure 8. Comparing the average $k(= 3.70 \times 10^{-7}$ m^2 s$^{-1})$ with $k(= 2.44 \times 10^{-7}$ m^2 s$^{-1})$ obtained by using equation (9) shows that equation (9) underestimates k, directly causing an overestimate of the phase shift of soil temperature from equation (2).

4.4. Modeling Soil Temperatures for Two Deeper Layers

[31] As mentioned above, k is estimated to be 6.54×10^{-7} m^2 s^{-1} and 2.55×10^{-7} m^2 s^{-1}, and W is estimated to be 1.01×10^{-6} m s^{-1} and -2.40×10^{-6} m s^{-1} (where minus means that $\partial k/\partial z < 0$) by using equations (5) and (6) for the two soil layers: $0.10-0.20$ m, and $0.20-0.40$ m in depth, respectively. It is obvious that both k and W changed significantly with increasing soil depth. We also model the soil temperature at 0.20 m and 0.40 m depths using equation (4), and the results are in satisfactory agreement with direct measurements as shown in Figure 9.

[32] We recommend using equation (4) instead of equation (2) for estimating soil temperature. However, when equation (4) is applied in land surface models, M and N (or equivalently k and W) are difficult to obtain. This problem also occurs in obtaining k from current land surface models, such as SiB2 where W is not used. To solve this problem, SiB2 parameterizes k by using soil volumetric water content [*Sellers et al.*, 1996]. We here physically characterize M and N (or equivalently k and W) to aid in future work. Furthermore, the latest land surface model, the Common Land Model (CLM) from NCAR, uses a layered numerical soil scheme which allows for heterogeneity imposed by vertical variation of porosity, texture, and soil moisture in the terms of the diffusion equation [*Dai et al.*, 2003].

5. Conclusions

[33] Two algorithms for soil temperature estimation have been theoretically analyzed and experimentally compared.
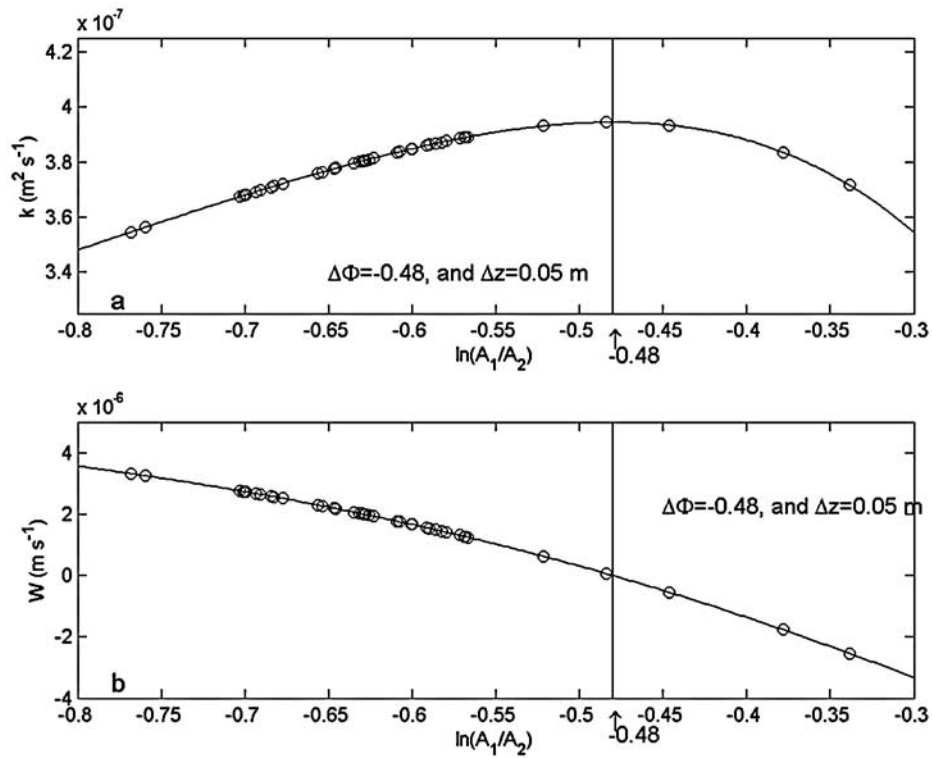
Figure 7. Variation of (a) soil thermal diffusivity k (m^2 s^{-1}) and (b) $W(= \frac{\partial k}{\partial z} - \frac{C_W}{C_g}w\theta)$ (m s^{-1}) versus $\ln(A_1/A_2)$ when the soil temperature phase shift $\Delta\Phi$ (rad) is fixed to be -0.48.

The traditional algorithm assumes that soil is vertically homogenous and takes into account only thermal conduction, whereas the new algorithm considers the vertical heterogeneity in soil and incorporates the impact of upward thermal convection (i.e., water transport) on soil temperature. The main shortcoming of the traditional algorithm is that it overestimates both the amplitude and the phase shift of the soil temperature when the vertical gradient of soil
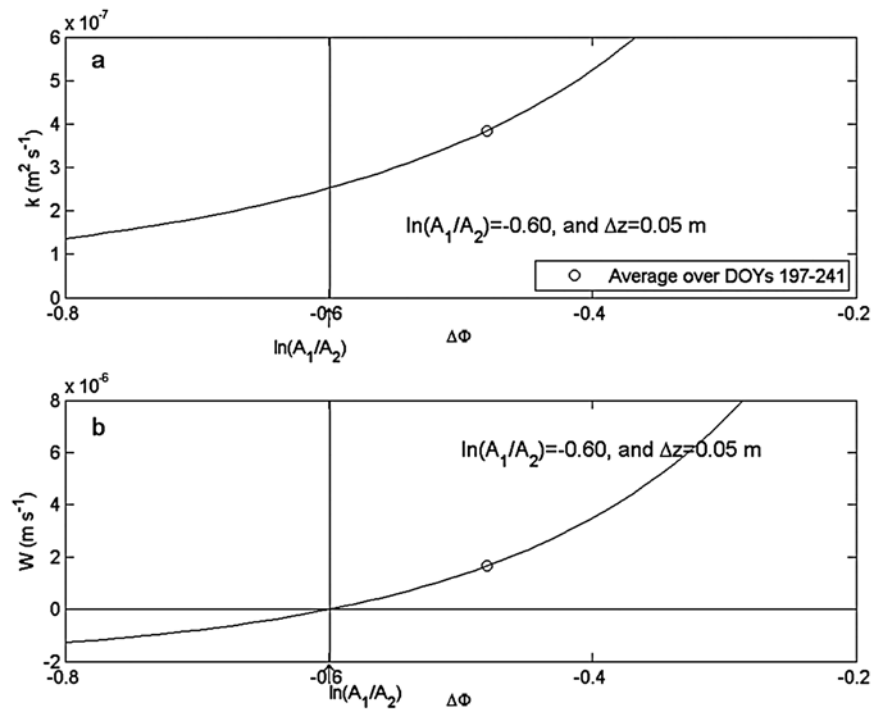

Figure 8. Variations of (a) soil thermal diffusivity k (m^2 s^{-1}) and (b) $W(= \frac{\partial k}{\partial z} - \frac{C_W}{C_g}w\theta)$ (m s^{-1}) against soil temperature phase shift $\Delta\Phi$ (rad) when $\ln(A_1/A_2)$ is fixed to be -0.60.
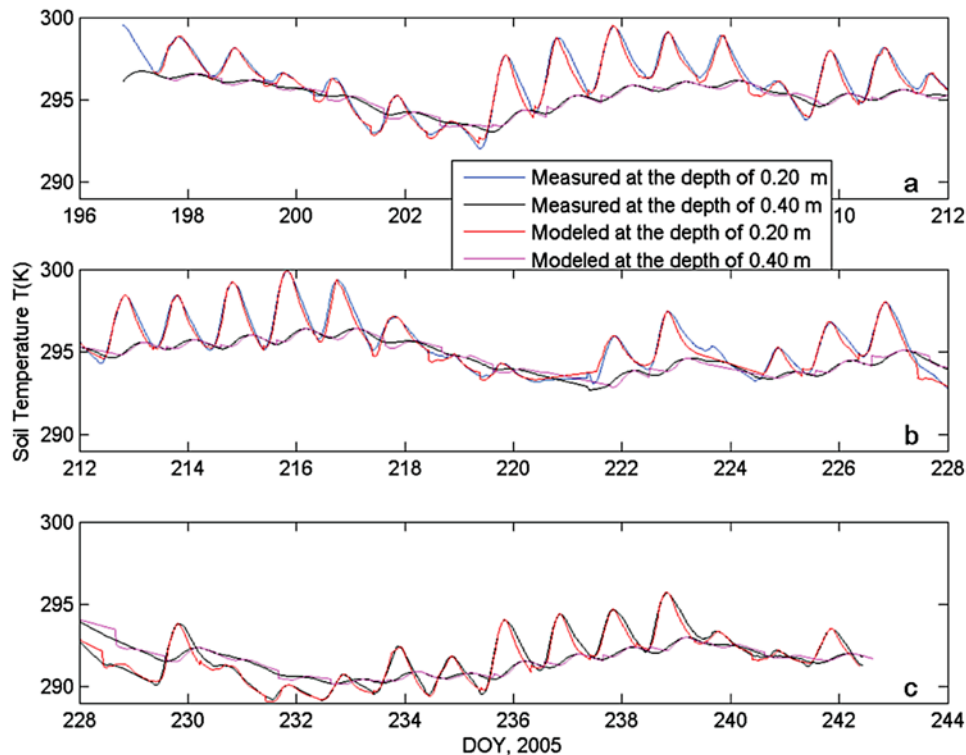
Figure 9. Comparison of soil temperature modeled by using equation (4) where ($W \neq 0$) with the observed temperatures at two depths, 0.20 and 0.4 m, from DOY 197 to DOY 241, 2005.

thermal diffusivity is large, and/or vertical water movement in the soil is not negligible. The traditional method produces a realistic estimate of soil temperature only for vertically homogenous dry soils.

[34] The analytical procedure proposed here to examine k and W should help in coupling soil water and heat numerical procedures in hydrologic models. The results show that the modeled soil temperature is very sensitive to soil thermal diffusivity and to its vertical gradient. For the study site, the results show that k and W decrease with increasing soil depth.

[35] We found that the new model gives better agreement with observations on the Loess Plateau in China than the traditional model. Further testing of this algorithm over other types of land surfaces is in progress.

References

Dai, Y., et al. (2003), The common land model (CLM), *Bull. Am. Meteorol. Soc.*, *84*, 1013–1023, doi:10.1175/BAMS-84-8-1013.

Gao, Z. (2005), Determination of soil heat flux in a Tibetan short-grass prairie, *Boundary Layer Meteorol.*, *114*, 165–178, doi:10.1007/s10546-004-8661-5.

Gao, Z., X. Fan, and L. Bian (2003), An analytical solution to one-dimensional thermal conduction-convection in soil, *Soil Sci.*, *168*, 99–107, doi:10.1097/00010694-200302000-00004.

Garratt, J. R. (1992), *The Atmospheric Boundary Layer*, 316 pp., Cambridge Univ. Press, Cambridge, U.K.

Heusinkveld, B. G., A. F. G. Jacobs, A. A. M. Holtslag, and S. M. Berkowicz (2004), Surface energy balance closure in an arid region: Role of soil heat flux, *Agric. For. Meteorol.*, *122*, 21–31, doi:10.1016/j.agrformet.2003.09.005.

Holmes, T. R. H., M. Owe, R. A. M. Jeu De, and H. Kooi (2008), Estimating the soil temperature profile from a single depth observation: A simple empirical heatflow solution, *Water Resour. Res.*, *44*, W02412, doi:10.1029/2007WR005994.

Horton, R., P. J. Wierenga, and D. R. Nielsen (1983), Evaluation of methods for determination apparent thermal diffusivity of soil near the surface, *Soil Sci. Soc. Am. J.*, *47*, 23–32.

Karam, M. A. (2000), A thermal wave approach for heat transfer in a nonuniform soil, *Soil Sci. Soc. Am. J.*, *64*, 1219–1225.

Lin, J. D. (1980), On the force-restore method for prediction of ground surface temperature, *J. Geophys. Res.*, *85*(C6), 3251–3254, doi:10.1029/JC085iC06p03251.

Massman, W. J. (1993), Periodic temperature variations in an inhomogeneous soil: a comparison of approximate and analytical expressions, *Soil Sci.*, *155*, 331–338, doi:10.1097/00010694-199305000-00004.

Massman, W. J., and J. M. Frank (2004), The effect of a controlled burn on the thermophysical properties of a dry soil using a new model of soil heat flow and a new high temperature heat flux sensor, *Int. J. Wildland Fire*, *13*, 427–442, doi:10.1071/WF04018.

Massman, W. J., J. M. Frank, and N. B. Reisch (2008), Long term impacts of controlled burns on soil thermal conductivity and soil heating at a Colorado Rocky Mountain site: A data/model fusion study, *Int. J. Wildland Fire*, *17*(1), 131–146, doi:10.1071/WF06118.

Nerpin, S. V., and A. F. Chudnovskii (1984), *Heat and Mass Transfer in the Plant-Soil-Air System*, Oxonian, New Delhi.

Novak, M. D. (1986), Theoretical values of daily atmospheric and soil thermal admittances, *Boundary Layer Meteorol.*, *34*, 17–34, doi:10.1007/BF00120906.

Novak, M. D. (1991), Analytical solutions to predict the long-term surface energy balance components and temperature of a bare soil, *Water Resour. Res.*, *27*, 2565–2576, doi:10.1029/91WR01637.

Passerat de Silans, A. M. B., B. A. Monteny, and J. P. Lhomme (1996), Apparent soil thermal diffusivity, a case study: HAPEX-Sahel experiment, *Agric. For. Meteorol.*, *81*, 201–216, doi:10.1016/0168-1923(95)02323-2.

Randall, D. A., et al. (1996), A revised land surface parameterization (SiB2) for atmospheric GCMs. Part III: The greening of the Colorado State University general circulation model, *J. Clim.*, *9*, 738–763, doi:10.1175/1520-0442[1996]009<0738:ARLSPF>2.0.CO;2.

Ren, T., G. J. Kluitenburg, and R. Horton (2000), Determining soil water flux and pore water velocity by a heat pulse technique, *Soil Sci. Soc. Am. J.*, *64*, 552–560.

Sellers, P. J., D. A. Randall, G. J. Collatz, J. A. Berry, C. B. Field, D. A. Dazlich, C. Zhang, G. D. Collelo, and L. Bounoua (1996), A revised land surface parameterization (SiB2) for atmospheric GCMs. Part I: Model formulation, *J. Clim.*, *9*, 676–705, doi:10.1175/1520-0442[1996]009<0676:ARLSPF>2.0.CO;2.

Shao, M., R. Horton, and D. B. Jaynes (1998), Analytical solution for one-dimensional heat conduction-convection equation, *Soil Sci. Soc. Am. J.*, *62*, 123–128.

Van Wijk, W. R., and D. A. deVries (1963), Periodic temperature variations in a homogeneous soil, in *Physics of Plant Environment*, edited by W. R. van Wijk, pp. 103–143, North-Holland, Amsterdam.

Verhoef, A. (2004), Remote estimation of thermal inertia and soil heat flux for bare soil, *Agric. For. Meteorol.*, *123*, 221–236, doi:10.1016/j.agrformet.2003.11.005.

Verhoef, A., J. J. M. B. van den Hurk, A. F. G. Jacobs, and B. G. Heusinkveld (1996), Thermal soil properties for a vineyard (EFEDA-I) and a savanna (HAPEX-Sahel) site, *Agric. For. Meteorol.*, *78*, 1–18, doi:10.1016/0168-1923(95)02254-6.

Wang, Y. (2004), A study on response of arid over China loess plateau to global change (in Chinese with English abstract) (online), *Sci. J. Northwest Univ. Online*, *2*(8), pap. 90.

Wei, Z., J. Wen, S. Lu, S. Chen, Y. Ao, and L. Liang (2005), A primary field experiment of land-atmosphere interaction over the Loess Plateau and its ground surface energy in clear days (in Chinese with English abstract), *Plateau Meteorol.*, *24*(4), 545–555.

————————————

Z. Gao and L. Wang, State Key Laboratory of Atmospheric Boundary Layer Physics and Atmospheric Chemistry, Institute of Atmospheric Physics, CAS, Beijing 100029, China.

R. Horton, Department of Agronomy, Iowa State University, Ames, IA 50011-1010, USA.

D. H. Lenschow, National Center for Atmospheric Research, 1850 Table Mesa Drive, Boulder, CO 80303, USA. (lenschow@ucar.edu)

J. Wen, Cold and Arid Regions Environmental and Engineering Research Institute, CAS, Lanzhou 730000, China.

M. Zhou, Key Laboratory for Polar Science, Polar Research Center of China, Shanghai 200129, China.